

BOND-SLIP MODELS FOR FRP SHEET/PLATE-TO-CONCRETE INTERFACES

X.Z. Lu¹, J.G. Teng², L.P. Ye¹ and J.J. Jiang¹

¹ Department of Civil Engineering, Tsinghua University, Beijing, PR China

² Department of Civil and Structural Engineering,

The Hong Kong Polytechnic University, Hong Kong, PR China

Abstract: A meso-scale finite element model is first presented for simulating the debonding behavior of FRP-to-concrete bonded joints in simple shear tests. In this model, both the FRP plate/sheet and the concrete are modeled using elements of mesoscopic sizes so that the shapes and paths of cracks during the entire debonding process can be appropriately captured. Results obtained from this model are next presented to provide insight into the debonding failure process. Finally, based on a finite element parametric study and existing test results, three bond-slip models of different levels of sophistication are presented. These proposed models are far more accurate than all existing bond-slip models.

1 INTRODUCTION

External bonding of fiber reinforced polymer (FRP) plates or sheets has emerged as a popular method for the strengthening of reinforced concrete (RC) structures. In this strengthening method, the performance of the FRP-to-concrete interface in providing an effective stress transfer is of crucial importance. Indeed, a number of failure modes in FRP-strengthened RC members are directly caused by debonding of the FRP from the concrete. Therefore, for the safe and economic design of externally bonded FRP systems, a sound understanding of the behavior of FRP-to-concrete interfaces needs to be developed and a reliable bond-slip model established. It should be noted that term “interface” in this paper represents the adhesive and the adjacent concrete responsible for the relative slip between the FRP plate/sheet and the concrete prism except when it is used in the phrase “concrete-to-adhesive interface” to refer to the physical interface.

In various debonding failure modes, the stress state of the interface is similar to that in a shear test

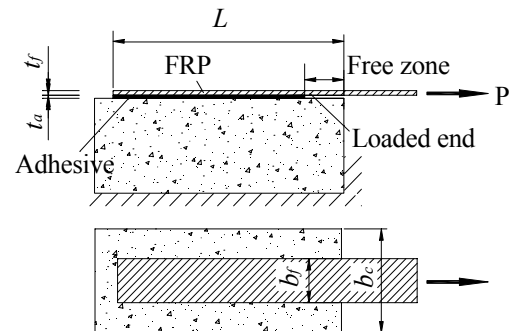


Figure 1. Shear test specimen

specimen in which a plate is bonded to a concrete prism and is subject to tension (Figure 1). As a result, a large number of studies, both experimental and theoretical, have been carried out on simple shear tests on bonded joints. Existing studies suggest that the main failure mode of FRP-to-concrete bonded joints in shear tests is concrete failure under shear, occurring generally at a few millimeters from the concrete-to-adhesive interface [1]. The ultimate load (i.e. the maximum transferable load) of the joint therefore depends strongly on the strength of concrete. In addition, the plate-to-concrete member width ratio also has a significant effect. A very important aspect of the behavior of these bonded joints is that there exists an effective bond length beyond which an extension of the bond length cannot increase the ultimate load. This is a fundamental difference between an externally bonded plate and an internal reinforcing bar for which a sufficiently long anchorage length can always be found so that the full tensile strength of the reinforcement can be achieved.

Existing research has also led to a number of bond stress-slip models based on the direct interpretation of results from shear tests [2,3]. These models suffer from the large scatter generally associated with such test data and also often from the limitation of the test data available to the researchers. As a result, none of them has been found to be of sufficient accuracy when assessed using a large test database [3]. This paper therefore presents a group of new bond-slip models developed in a recent study reported in detail in Ref. [3]. Instead of relying exclusively on test data, a meso-scale finite element model was first developed and employed to establish the various relationships between the bond parameters and the geometric and material parameters of FRP-to-concrete bonded joints. The derived relationships were then fine-tuned through calibration with a large test database. In the following sections, the meso-scale finite element model is first presented, which is then followed by an exploration of the failure mechanism using this model. Three bond-slip models of different levels of sophistication are finally presented and their predictions compared with test results.

2. MESO-SCALE FINITE ELEMENT MODEL

2.1 General considerations

In general, the debonding of FRP from concrete occurs within a thin layer of concrete adjacent to the concrete-to-adhesive interface unless the adhesive is rather weak. The thickness of this concrete layer is about 2~5mm. To simulate concrete failure within such a thin layer, with the shapes and paths of the cracks properly captured, the rotating angle crack model (RACM) [4,5] should be used if elements with a size comparable to the thickness of the concrete layer are adopted. The RACM however has the major drawback that its crack surface parameters have to be empirically derived from the shear tests. Therefore, the present study employed a fixed angle crack model (FACM)[5] in conjunction with a very fine finite element mesh with element sizes being one order smaller than the thickness of the failure zone of concrete. This approach has the simplicity of the FACM for which the relevant material parameters have clear physical meanings and can be found from well established standard tests, but in the meantime retains the capability of tracing the paths of cracks as deformations increase. The

present model using very small elements is referred to as the meso-scale finite element model. To reduce the computational effort, the three-dimensional FRP-to-concrete bonded joint (Figure 1) was modeled as a plane stress problem using 4-node isoparametric elements. The effect of FRP-to-concrete width ratio was separately considered based on the work of Chen and Teng [1].

It should be noted that the present model differs from those employed in existing finite element studies of FRP-to-concrete bond behavior in which an interface element is employed to simulate debonding [e.g. 6,7]. In such models, the interface element has to be based on a bond-slip model which needs to be pre-defined. Such models are not true predictive models, although they may be used with test data to verify/identify interfacial behavior. The present model has the capability of predicting the interfacial behavior from first principles.

2.2 Modeling of FRP

As the element size adopted in this study was within the range of 0.25~0.5mm, the FRP plate was modeled with plane stress elements. The use of plane stress elements simplified the modeling procedure in terms of proper interaction between the FRP and concrete. The FRP plate/sheet was treated as an isotropic material.

2.3 Modeling of concrete

When concrete is modeled using small elements (here element sizes of 0.25~0.5mm), the element size effect should be considered. According to Bazant [8], the compressive behavior of concrete does not depend significantly on element sizes, so the stress-strain relationship proposed by Hognestad [9] was directly used in the present study to simulate the compressive behavior of concrete.

The tensile behavior of concrete was modeled using the crack band model [8]. The essence of this approach is to control the post-cracking softening branch of the tensile stress-strain curve using the concept of fracture energy in which element sizes are considered. For the linear softening model proposed by Hillerborg, the ultimate tensile strain ε_{cr}^u at which the tensile stress decreases to zero is given by [10]

$$\varepsilon_{cr}^u = 2G_f^I / (b_{cr} f_t) \quad (1)$$

where G_f^I is the fracture energy of concrete; f_t is the tensile strength of concrete; and b_{cr} is the crack band width (ie the element size). According to the model code of

CEB-FIP [11], $G_f^I = \alpha(f_c / 10)^{0.7}$, where f_c is the compressive strength of concrete.

For concrete of normal aggregate size, $\alpha = 0.03$ [11].

The modeling of the shear behavior of cracked concrete also needs to take into account the effect of element size. Eight different shear models for cracked concrete were compared in the present study, which identified the following model developed at Dalian University of Technology [12] in China as the best performing model [2]:

$$\tau = (0.543w^{-0.585} + 0.1999)\sqrt{f_c}\Delta^{0.72} \quad (2)$$

where w is the crack width and Δ is the relative slip between the crack surfaces, both in mm. Equation (2) was therefore adopted to model the shear behavior of cracked concrete in the present study.

2.4 Implementation

The concrete model described above was implemented into the general purpose finite element package MSC. MARC [13] as a user subroutine.

Before finalizing the finite element model, a number of issues were first examined for accurate predictions, including the post-peak softening scheme and the element size [2]. The final finite element model employed an element size of 0.5mm, with a linear softening branch for concrete subject to tension.

The finite element model was verified by detailed comparison with the results of 12 shear test specimens [2]. A close agreement was achieved for all 12 specimens. A typical comparison of the distribution of longitudinal strain on the FRP plate is shown in Figure 2.

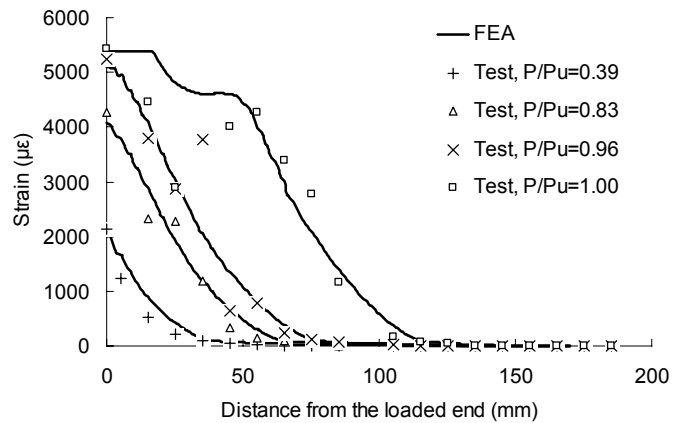


Figure 2. Comparison of strain distributions in the FRP sheet

3. DEBONDING PROCESS

The process of crack propagation is difficult to observe in laboratory tests but can be easily predicted by the finite element model. It should however be noted that the actual process of debonding is more complicated than is predicted by the present model, as real concrete is an inhomogeneous material. Nevertheless, the present finite results provide useful insight into the failure mechanism.

Figure 3 shows a set of diagrams of crack strain (total tensile strain minus elastic strain) contours corresponding to different slips at the loaded end. The state each diagram represents can be identified by comparing its slip at the loaded end to the slip value s_0 when the local bond strength is reached at the loaded end and s_f when the ultimate load P_u is first attained. For this specimen, $s_0 = 0.0585$ mm, and $s_f = 0.154$ mm.

Figure 3a shows that even at a load of 28% of the ultimate load, the concrete under the FRP plate near the loaded end has experienced extensive cracking. The cracks can be classified into 3 types: (a) interfacial shallow cracks; (b) interfacial deep cracks; and (c) micro-cracks within a cracked zone under the FRP plate. The same three types of cracks also exist at later stages of deformation as shown in Figure 3b~e.

The depths of the interfacial shallow cracks are about 0.5~1mm, whose widths are small and relatively uniform. This thin layer is subject to high tensile stresses as well as

high shear stresses as it is directly bonded to the FRP. The depths of the interfacial deep cracks are 2~5mm. The widths of these cracks are relatively large. They are caused by shear stresses and will control the final debonding strength and the slip of the interface. The overall depth of the cracked zone of concrete is about 5~10mm. They are also caused by shear stresses and some will develop into interfacial deep cracks as deformation further increases.

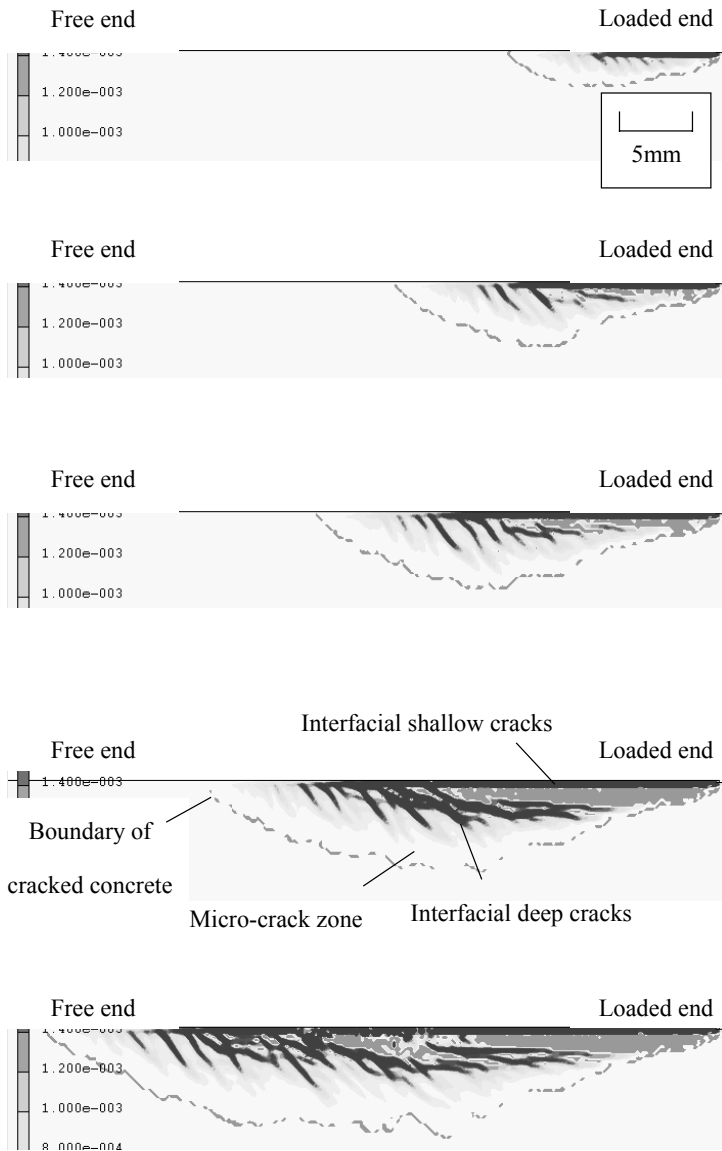


Figure 3. Propagation of cracks in concrete

The above classification of crack patterns also helps explain the failure process. At a low level of loading, the formation of interfacial shallow cracks at angles of 45~60° to the interface leads to the appearance of small cantilever columns (i.e. meso-cantilevers). With further increases in loading, these cantilevers may grow longer as the shallow cracks grow into deep cracks or may fail if the shear force acting on the cantilever reaches a critical value. The shear force F on the cantilever leads to axial compressive

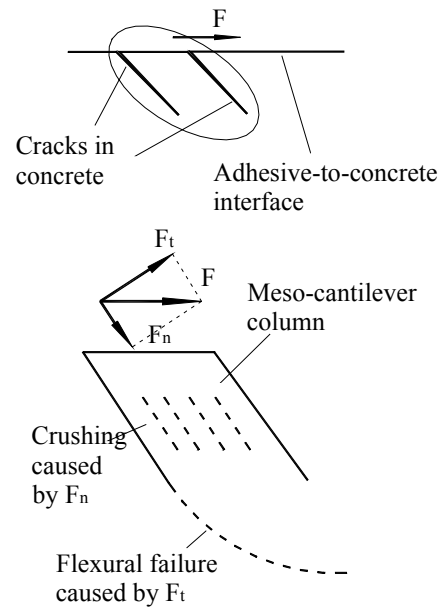


Figure 4. Meso-cantilever column and its failure modes

stresses which can cause crushing failure, or flexural tensile stresses at the root which is responsible for flexural failure at the root (Figure 4). It is worth noting that debonding as observed in laboratory tests corresponds to the progressive flexural failure of the meso-cantilevers, except near the loaded end where debonding is mainly due to the crushing of the meso-cantilevers.

4 LOCAL BOND -SLIP MODELS

4.1 General

The finite element model, following verification, was deployed to study the local bond-slip behavior as from such a model, the stress in and the slip of the FRP plate at any point along the plate under any level of loading can be obtained easily. The interfacial shear stress can be deduced from the longitudinal stresses in the FRP plate. Due to localization of cracks, the deduced shear stresses show substantial local fluctuations so a smoothing procedure was applied [3]. A typical bond-slip curve obtained from this procedure is shown in Figure 5, where E_f is the elastic modulus of FRP plate, G_a and t_a are the shear modulus and thickness of the adhesive layer, respectively.

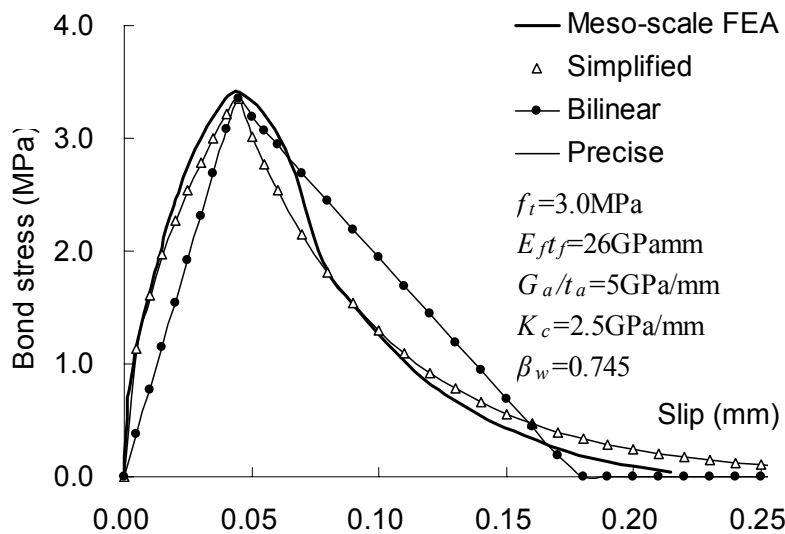


Figure 5. Bond-slip curves

In order to develop bond-slip models, a finite element parametric study was carried out to establish the relationships between various bond parameters and geometric and material parameters. This parametric study showed that the local bond strength τ_{\max} and the corresponding slip s_0 are almost linearly related to the tensile strength of concrete f_t , while the total interfacial fracture energy G_f is almost linearly related to $\sqrt{f_t}$. Based on such finite element bond-slip curves and some calibration with a large test database, three bond-slip models were developed [3].

4.2 Precise model

The first of the three bond-slip models is referred to as the precise model as it takes explicit account of the effect of the adhesive layer, which is important when the adhesive is much softer than those currently in common use. It has been reported that very soft adhesive layers can increase the interfacial fracture energy [14]. The prediction of the precise model is almost identical to that of the simplified model presented below for normal adhesives.

The precise model describes the ascending and descending branches separately using the following equations:

$$\tau = \tau_{\max} \left(\sqrt{\frac{s}{s_0 A} + B^2} - B \right) \quad \text{if } s \leq s_0 \quad (3a)$$

$$\tau = \tau_{\max} \exp[-\alpha(s/s_0 - 1)] \quad \text{if } s > s_0, \quad (3b)$$

where $A = (s_0 - s_e)/s_0$, $B = s_e/[2(s_0 - s_e)]$

The local bond strength τ_{\max} and the corresponding slip s_0 are given by

$$\tau_{\max} = 1.5\beta_w f_t \quad (3c)$$

$$s_0 = 0.0195\beta_w f_t + s_e \quad (3d)$$

where $s_e = \tau_{\max}/K_0$ is the elastic component of s_0 and the FRP-to-concrete width ratio β_w can be expressed as

$$\beta_w = \sqrt{(2.25 - b_f/b_c)/(1.25 + b_f/b_c)} \quad (3e)$$

with b_c and b_f being the widths of the concrete prism and the FRP plate respectively (Fig.1). The initial stiffness of the bond-slip model is defined by:

$$K_0 = K_a K_c / (K_a + K_c) \quad (3f)$$

where $K_a = G_a/t_a$ and $K_c = G_c/t_c$. G_c is the elastic shear modulus of concrete and t_c is the effective thickness of concrete whose deformation forms part of the interfacial slip and may be taken as 5mm unless this thickness is specifically measured during the test.

The parameter α controls the shape of the descending branch and is given by

$$\alpha = \tau_{\max} s_0 / (G_f - G_f^a) \quad (3g)$$

where the total interfacial fracture energy can be expressed as:

$$G_f = 0.308\beta_w^2 \sqrt{f_t} f(K_a) \quad (3h)$$

while the fracture energy of the ascending branch G_f^a can be calculated as:

$$G_f^a = \int_0^{s_0} \tau ds = \tau_{\max} s_0 \left[\frac{2A}{3} \left(\frac{1+B^2A}{A} \right)^{3/2} - B - \frac{2}{3} B^3 A \right] \quad (3i)$$

Here, $f(K_a)$ is a function of the stiffness of the adhesive layer. Based on finite element results, for normal adhesives with $K_a \geq 2.5 \text{ GPa/mm}$, the effect of adhesive layer stiffness on G_f is very small, so it is proposed that $f(K_a)=1$ for normal adhesives. A precise definition of $f(K_a)$ requires further work. The prediction of the precise model for an example FRP-to-concrete bonded joint is shown in Figure 5 and is seen to compare very well with the prediction of the meso-scale finite element analysis.

4.3 Simplified model

The precise model is accurate but complicated. For normal adhesives, a simplified model without a significant loss of accuracy can be easily obtained. This is because the initial stiffness of the bond-slip curve is much larger than the secant stiffness at the peak point when a normal adhesive of a reasonable thickness is used. Therefore, the initial stiffness can be approximated as infinity. Furthermore, the interfacial fracture energy G_f has little relationship with the stiffness of the adhesive layer. Based on these two simplifications, the following simplified bond-slip model can be obtained:

$$\left\{ \begin{array}{l} \tau = \tau_{\max} \sqrt{\frac{s}{s_0}} \quad \text{if } s \leq s_0 \end{array} \right. \quad (4a)$$

$$\left\{ \begin{array}{l} \tau = \tau_{\max} e^{-\alpha \left(\frac{s}{s_0} - 1 \right)} \quad \text{if } s > s_0 \end{array} \right. \quad (4b)$$

$$\text{where } s_0 = 0.0195 \beta_w f_t \quad (4c)$$

$$G_f = 0.308 \beta_w^2 \sqrt{f_t} \quad (4d)$$

$$\alpha = \frac{1}{\frac{G_f}{\tau_{\max} s_0} - \frac{2}{3}} \quad (4e)$$

and τ_{\max} and β_w can be found from Eq. 3(c) and 3(e).

The bond-slip curve of the example bonded joint predicted by the simplified model is also shown in Figure 5, where it can be seen that there is little difference between this model and the precise model as a normal adhesive is used in this bonded joint. For all practical purposes, the simplified model is sufficient for normal adhesive joints but much simpler than the precise model.

4.4 Bilinear model

Further simplification was made to the simplified model, leading to a simple bilinear model which can be used to derive an explicit design equation for the ultimate load. This bilinear model has the same local bond strength and total fracture energy, so the

ultimate load remains unchanged if the bond length is longer than the effective bond length. This bilinear model is described by the following equations:

$$\tau = \tau_{\max} s / s_0 \quad \text{if } s \leq s_0 \quad (5a)$$

$$\tau = \tau_{\max} (s_f - s) / (s_f - s_0) \quad \text{if } s_0 < s \leq s_f \quad (5b)$$

where $s_f = 2G_f / \tau_{\max}$ and τ_{\max} , s_0 and β_w can be found using Eq.3(c), 4(c) and 3(e). The prediction of the bilinear model is also shown in Figure 5 to illustrate the differences between this and the other two models.

Table 1 provides the statistics of comparisons of the ultimate load between the three proposed models and 254 shear test results. Very close agreements are seen. The strain distributions in the FRP sheet numerically predicted with the proposed bond-slip models are also in close agreement with test results. A typical comparison is shown in Figure 6 for Specimen PG1-2 tested by Tan [15]. Further extensive comparisons are available in Ref. [3] where it is demonstrated that the proposed models are far more accurate than all existing bond-slip models.

Table.1 Comparison of ultimate load between test results and proposed models

Model	Precise model	Simplified model	Bilinear model
Average error	0.1%	0.1%	0.1%
Standard deviation	0.155	0.155	0.156
Correlation coefficient	0.910	0	0.908

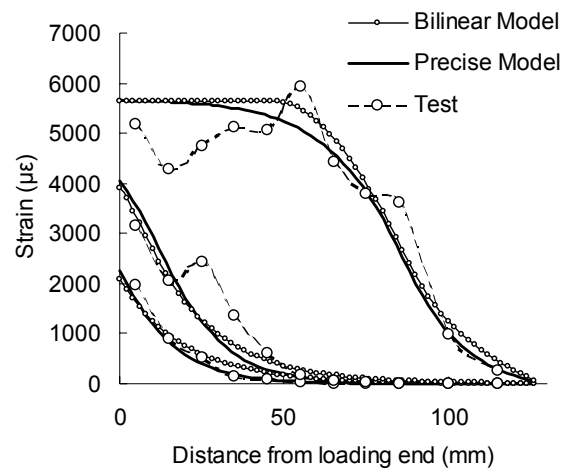


Figure 6. Comparison of strain distributions in the FRP sheet for Specimen PG1-2

5 CONCLUSIONS

A meso-scale finite element model has been proposed for the simulation of debonding behavior in FRP-to-concrete bonded joints and has been shown to produce accurate predictions. Results obtained from this model showed that debonding is due to the formation and failure of inclined meso-cantilever columns in the concrete. Based on a finite element parametric study and existing test results, three bond-slip models of different levels of sophistication have also been proposed. These proposed models are far more accurate than all existing bond-slip models.

6 ACKNOWLEDGEMENT

The authors gratefully acknowledge the financial support provided by the Natural Science Foundation of China (National Key Project No. 50238030) and The Hong Kong Polytechnic University through the Area

of Strategic Development (ASD) Scheme for the ASD in Mitigation of Urban Hazards

REFERENCES:

1. J F Chen and J G Teng, 'Anchorage strength models for FRP and steel plates bonded to concrete', *Journal of Structural Engineering, ASCE*, 2001 127(7) 784-791
2. X Z Lu, L P Ye, J G Teng and J J Jiang, 'Meso-scale finite element model for FRP sheets/plates externally bonded to concrete', in preparation.
3. X Z Lu, J G Teng, L P Ye and J J Jiang, 'Bond-slip models for FRP sheets/plates externally bonded to concrete', in preparation.
4. X Z Lu, Z Tan, L P Ye and J J Jiang, 'Finite element analysis for debonding in the interface between FRP sheet and concrete', *Engineering Mechanics*, 2003 in press
5. J G Rots and J Blaauwendraad, 'Crack models for concrete: discrete or smeared? Fixed, multi-directional or rotating?', *HERON*, 1989 34(1)
6. Z S Wu and J Yin, 'Fracture behaviors of FRP-strengthened concrete structures', *Engineering Fracture Mechanics*, 2003 70(10) 1339-1355
7. Z S Wu, *Element-level study on stress transfer based on local bond properties*, Technical Report of JCI Technical Committee on Retrofit Technology, 2003 44-56
8. Z P Bazant and J Planas, *Fracture and size effect in concrete and other quasibrittle materials*, Boca Baton, CRC Press, 1997.
9. E Hognestad, *A study of combined bending and axial load in reinforced concrete members*, University of Illinois Engineering Experiment Station, Bulletin Series No. 399, Bulletin No.1, 1951
10. J G Rots, P Nauta, M A Kusters and J Blaauwendraad, 'Smeared crack approach and fracture localization in concrete', *HERON*, 1985, 30(1)
11. CEB-FIP Committee, Model Code 90, Lausanne, 1993
12. Q L Kang, *Finite element analysis for reinforced concrete*, Beijing, China Water Power Press, 1996 120-126
13. *MSC.Marc User's Manual, Volume A (Theory and User Information)*, MSC. Software Corporation, 2003
14. J G Dai and T Ueda, 'Local bond stress slip relationship for FRP sheets-concrete interfaces', Proceedings of the 6th International Symposium on *FRP Reinforcement for Concrete Structures*, Singapore, World Scientific Press, 2003 143-152
15. Z Tan, *Experimental Research for RC Beam Strengthened with GFRP*, Master Dissertation, Beijing, Tsinghua University, 2002.